

# Experimental analysis of organ decay and pH gradients within a carcass and the implications for phosphatization of soft tissues

Clements, Thomas; Purnell, Mark A.; Gabbott, Sarah

DOI:

[10.1111/pala.12617](https://doi.org/10.1111/pala.12617)

License:

Creative Commons: Attribution (CC BY)

*Document Version*

Publisher's PDF, also known as Version of record

*Citation for published version (Harvard):*

Clements, T, Purnell, MA & Gabbott, S 2022, 'Experimental analysis of organ decay and pH gradients within a carcass and the implications for phosphatization of soft tissues', *Palaeontology*, vol. 65, no. 4, e12617. <https://doi.org/10.1111/pala.12617>

[Link to publication on Research at Birmingham portal](#)

## General rights

Unless a licence is specified above, all rights (including copyright and moral rights) in this document are retained by the authors and/or the copyright holders. The express permission of the copyright holder must be obtained for any use of this material other than for purposes permitted by law.

- Users may freely distribute the URL that is used to identify this publication.
- Users may download and/or print one copy of the publication from the University of Birmingham research portal for the purpose of private study or non-commercial research.
- User may use extracts from the document in line with the concept of 'fair dealing' under the Copyright, Designs and Patents Act 1988 (?)
- Users may not further distribute the material nor use it for the purposes of commercial gain.

Where a licence is displayed above, please note the terms and conditions of the licence govern your use of this document.

When citing, please reference the published version.




## Take down policy

While the University of Birmingham exercises care and attention in making items available there are rare occasions when an item has been uploaded in error or has been deemed to be commercially or otherwise sensitive.

If you believe that this is the case for this document, please contact [UBIRA@lists.bham.ac.uk](mailto:UBIRA@lists.bham.ac.uk) providing details and we will remove access to the work immediately and investigate.



# Experimental analysis of organ decay and pH gradients within a carcass and the implications for phosphatization of soft tissues

by THOMAS CLEMENTS<sup>1,2,\*</sup> , MARK A. PURNELL<sup>2</sup>  and SARAH GABBOTT<sup>2,\*</sup> 

<sup>1</sup>School of Geography, Earth & Environmental Sciences, University of Birmingham, Edgbaston, Birmingham, B15 2TT, UK; clements.taph@gmail.com

<sup>2</sup>Centre for Palaeobiology & Biosphere Evolution, School of Geography, Geology and the Environment, University of Leicester, University Road, Leicester, LE1 7RH, UK; clements.taph@gmail.com, sg21@leicester.ac.uk

\*Corresponding author

Typescript received 20 September 2021; accepted in revised form 14 April 2022

**Abstract:** Replacement of soft tissues by calcium phosphate can yield spectacular fossils. However, in the fossil record, the phosphatization of internal organs is highly selective; some internal organs, such as muscles, stomachs, and intestines, appear to preferentially phosphatize while other organs seldom phosphatize. The reasons for this are unclear but one hypothesis is that, during decay, organs create distinct chemical microenvironments and only some fall below the critical pH threshold for mineralization to occur (i.e. below the carbonic acid dissociation constant: pH 6.38). Here, we present a novel investigation using microelectrodes that record dynamic spatial and temporal pH gradients inside organs within a fish carcass in real time. Our experiments demonstrate that within a decaying fish carcass, organ-specific microenvironments are not generated. Rather, a pervasive pH environment forms within the body cavity which persists until integumentary failure. With no evidence

to support the development of organ-specific microenvironments during decay our data suggest other factors must control differential organ phosphatization. We propose, that when conditions are amenable, it is tissue biochemistry that plays an important role in selective phosphatization. Tissues with high phosphate content (and those rich in collagen) are most likely to phosphatize. Internal organs that typically have lower tissue-bound phosphate, including the integuments of the stomach and intestine, may require other sources of phosphate such as ingested phosphate-rich organic matter. If tissue biochemistry is the driver behind selective phosphatization, this may provide insights into other highly selective modes of soft-tissue preservation (e.g. pyritization).

**Key words:** taphonomy, phosphatization, soft-tissue fossil, fish, fossil, fossilization.

SOFT-TISSUE bearing fossils yield information about the biology, ecology and evolution of ancient organisms that is not available from skeletal remains alone; they are thus of significant scientific and public interest. However, to correctly interpret the information captured by such fossils, we must understand the processes of decay, maturation and preservation which led to their formation and the timescales over which these processes operate (Purnell *et al.* 2018).

In most conditions, soft tissues are typically lost rapidly post mortem due to decay and cellular autolysis. However, one mode of preservation that can preserve soft-tissue anatomy is authigenic mineralization, the replacement of tissues by minerals that precipitate and grow *in situ*. Whilst the post-mortem soft-tissue preservation may occur through mineralization by silicates, clays, pyrite and carbonates, it is replacement by calcium phosphate (phosphatization) that is widely regarded as the

form of mineralization that yields the highest fidelity of soft-tissue preservation (see Briggs (2003) for a review; Fig. 1). Generally, during the process of soft-tissue phosphatization, minute crystals of apatite (*c.* <30 nm) form on and within the decaying tissue substrates and can faithfully replicate morphology on a cellular and even subcellular level (Martill 1988; Wilby 1993). However, there are controls on phosphatization that remain poorly understood. Decay experiments have revealed important information on the chemical conditions that promote phosphate precipitation (Briggs *et al.* 1993; Briggs & Kear 1994; Sagemann *et al.* 1999 *et al.*) demonstrating that pH is a fundamental control on phosphatization. In a marine environment, both calcium carbonate and calcium phosphate have been shown to precipitate in association with decaying organic matter (Briggs & Kear 1993, 1994; Briggs & Wilby 1996; Wilby & Briggs 1997) but typically it is only calcium phosphate that replicates soft-tissue

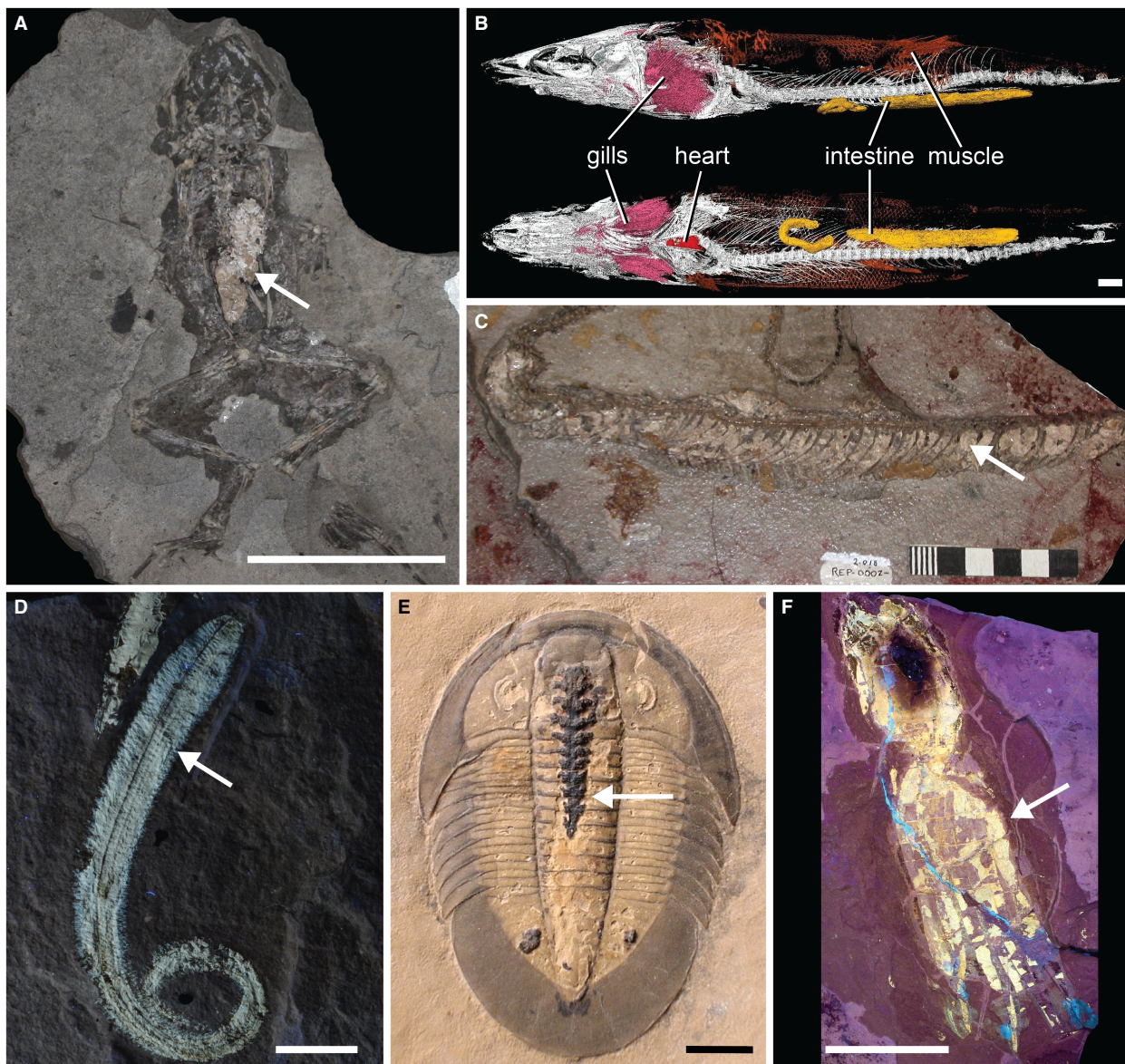


**FIG. 1.** Examples of phosphatized soft-tissues (arrowed). A, frog, *Pelophylax pueyoi* (MNCN 63805), with phosphatized void fill within the stomach, Miocene, Libros, Spain; image reproduced with permission from Maria McNamara (McNamara *et al.* 2012). B, synchrotron micro-CT image of left lateral view (above) and ventral view (below) of *Rhacolepis buccalis* (CNPEM 27P), within concretion, Cretaceous, Santana, Brazil; labelled internal organs are replaced by calcium phosphate; imaged using synchrotron radiation microtomography (PPC-SR-  $\mu$ CT); image reproduced with permission from Vincent Fernandez and José Xavier-Neto (Maldanis *et al.* 2016). C, colubrid snake, *Colubridae* indet. (MNCN 66503), with phosphatized skin, Miocene, Libros, Spain; image reproduced with permission from Maria McNamara (McNamara *et al.* 2016). D, polychaete worm, *Rollinschaeta myoplana* (NHMUK PI AN 15075), with phosphatized musculature, Cretaceous, Hakel and Hjoula, Lebanon; image reproduced with permission from Paul Wilson (Wilson *et al.* 2016). E, trilobite, *Meniscopsia beebeyi* (BPM 1017), with phosphatized intestinal tract, Cambrian, Weeks Formation, Utah, USA; image reproduced with permission from Rudy Lerosey-Aubril (Lerosey-Aubril *et al.* 2012). F, vampyropod octopus *Keupia* sp. (NHMUK PI CC 578A), Cretaceous, Hakel and Hjoula, Lebanon; specimen is photographed under ultraviolet light which causes phosphatized tissues to fluoresce in yellow; photo courtesy of Jonathan Jackson, NHMUK. Scales bars represent: 50 mm (A, B, F); 10 mm (E, D); C: one square = 10 mm.

morphology (Briggs & Kear 1994). In environments where  $\text{Ca}^{2+}$  and  $\text{PO}_4^{3-}$  ions are in sufficient abundance, the pH around a carcass must fall below the carbonic

dissolution constant (pH 6.38) for phosphatization to proceed, otherwise calcium carbonate precipitates (Briggs & Wilby 1996). This reduction in pH is driven by

bacterial respiration and cellular autolysis of organic matter which generates acidic by-products, such as CO<sub>2</sub> (aq), volatile fatty acids, and sulfuric acid (H<sub>2</sub>SO<sub>4</sub>) (Sagemann *et al.* 1999; McNamara *et al.* 2009). Environmental conditions are required that prevent decay products (including phosphorous) from diffusing away from the carcass, allowing a pronounced and sustained drop in pH to form (Briggs & Kear 1994; Wilby & Whyte 1995; Wilby *et al.* 1996; Iniesto *et al.* 2015); for example burial in sediment or overgrowth by a microbial mat (e.g. Iniesto *et al.* 2015). We know from the distribution of the occurrence of phosphatized soft tissues that suitable conditions can be met in a wide variety of depositional settings, and in different sediment types (Fig. 1). For example, phosphatized soft tissues are known from marine shelves (Martill 1988; Wilby & Briggs 1997; Fuchs *et al.* 2016; Wilson *et al.* 2016), shoals (Wilby & Whyte 1995), shallow epeiric seas (Allison 1988; Wilby & Briggs 1997; Wilby *et al.* 2004), lacustrine and other freshwater systems (Duncan *et al.* 1998; Arena 2008; McNamara *et al.* 2009); in siliciclastic silts and muds (e.g. Wilby *et al.* 2004) through to carbonates (e.g. Wilby & Whyte 1995). However, within any deposit where phosphatization occurs, not all taxa are captured through this taphonomic mode. For example, vertebrates, fish, worms and arthropods are more commonly preserved through phosphatization than other groups (Briggs & Wilby 1996; Table S1). Moreover, within these fossil groups there are anatomical features that are frequently fossilized through phosphatization, whereas others are not. This selective phosphatization appears to operate at the organ level; within individual fossil specimens the stomachs, intestines and musculature are commonly captured by calcium phosphate (by tissue replication, void fill, or both) while the liver, gonads and kidneys are seldom phosphatized (e.g. Martill 1988; Butterfield 2002; Etter & Tang 2002; McNamara *et al.* 2009; Fuchs *et al.* 2016; Wilson *et al.* 2016; Table S1). It is this organ-scale preservation bias that is the subject of this research.

Currently, it is unclear why selective phosphatization of organs occurs in the fossil record and what controls this bias. There are two major possibilities: (1) differences in organ decay rate; and (2) differences in biochemical composition of organs. Although these factors are linked, differences in the biochemical composition of organs are frequently cited as being the driving factor for selective preservation (e.g. McNamara *et al.* 2009; Lerosey-Aubril *et al.* 2012; Wilson *et al.* 2016; Clements *et al.* 2017; Saleh *et al.* 2020). One hypothesis is that the varying composition of internal organs contributes to the generation of highly localized geochemical conditions within a carcass during decay (i.e. organ specific pH microenvironments) (e.g. Briggs & Wilby 1996; Sagemann *et al.* 1999; McNamara *et al.* 2009). This hypothesis is supported by

investigations of fossil material and decay experiments that indicate that the influence of pH may be highly localized during decay (i.e. different minerals may form in different areas within the same carcass) and it may be dynamic (phosphatized tissues may be overgrown by later calcium carbonate) (Briggs & Wilby 1996; Sagemann *et al.* 1999). If this hypothesis is correct, it suggests that, during decay, the pH of some organs falls below the carbonic dissolution constant allowing calcium phosphate precipitation, while other organs do not generate suitable pH for phosphatization to occur. Therefore, documenting pH gradients associated with the decay of specific anatomical features may reveal why fossils show 'selective phosphatization' of some internal tissues and anatomy. However, this has never been experimentally tested because, until now, experiments investigating decay-induced pH variations have been restricted to recording pH fluctuations external to the carcass (e.g. Sagemann *et al.* 1999; Clements *et al.* 2017).

Here, we present the first use of microelectrodes inside specific organs within a carcass to document the real-time spatial and temporal pH gradients associated with decaying fishes. We test the null hypotheses that pH generated within a carcass is the same as that recorded outside it, and that internal organs do not generate distinct pH gradients during decay (see Fig. 2). The results of our experiment show that organs do not generate unique pH microenvironments during decay, and we discuss other factors that may control selective soft-tissue phosphatization and underline the importance of understanding both decay and preservation when interpreting exceptionally-preserved fossils.

## MATERIAL AND METHOD

### *Experimental design*

European sea bass (*Dicentrarchus labrax*) was chosen for analysis because of its availability and large size (making inserting pH probes into organs easier and more accurate). All specimens were adults of approximately similar size (>25 cm length). Adult European sea bass have limited external sexual dimorphism, making determination of the sex of the fish difficult prior to the commencement of the experiment. The fish were purchased from a local fishmonger (as soon after death as possible); they were kept on ice to retard decay, but to avoid cellular damage they were not frozen. We estimate that the interval between death and the start of the experiment was no more than 24–36 h (as estimated by the fish seller).

The experiment was undertaken in two parts: a primary experiment that logged the pH of the internal organs through decay, and a secondary experiment that

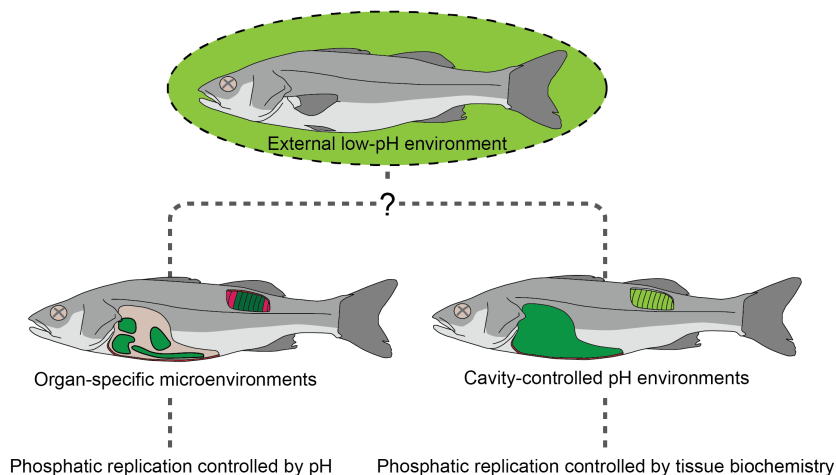


**FIG. 2.** Two hypotheses regarding the control on selective internal soft-tissue phosphatization. Experiments on several taxa have demonstrated that if diffusion of decay products is restricted during decay, a low-pH microenvironment forms around the carcass. However, it is not currently understood why some internal organs have a higher propensity for phosphatic preservation than others. One hypothesis is that the decaying internal organs form their own distinct pH microenvironment which may influence their likelihood of phosphatization (bottom left). Alternatively, if distinct body cavities (e.g. the coelom and dorsal muscle cavity) allow pervasive pH environments to form (bottom right), other factors, such as tissue biochemistry, are likely to be the major control. Our data indicate that the latter model is more likely.

allowed the morphology of decaying fish to be catalogued.

The primary experiment ( $n = 4$ ) was designed using Lazar PHR-146XS-7C pH probes (accuracy:  $\pm 0.01$  pH). The probes have a 2.8 mm diameter inert fluoropolymer body with a 1 mm diameter solid state sensor. Before the primary experiment was started, we undertook probe placement trials on six sea bass specimens. The following target organs were intended to be probed (Fig. 3A): the stomach, liver, intestines and epaxial muscle (a fifth probe was placed externally to the carcass approximately 1–2 mm away from the dermis). All the incisions were approximately 1–2 mm in length and were made using sterile scalpel blades (Fig. 3B). These trial runs showed, for example, that to insert the probe reliably into the stomach (herein probe 1) the best method was to make an incision between 5–8 mm posteriorly of the apex of the operculum and 1–2 mm below the lateral line. Probe 2 targeted the liver, approximately 5 mm below where the posterior edge of the pectoral fin connects to the dermis. Any ribs exposed by the incision were cut with scissors, to reduce the possibility of probe damage. The trial runs also demonstrated that the intestine of sea bass (midgut/hindgut) is difficult to probe accurately due to its small diameter and because the lateral orientation of the carcass in the experimental set-up (see Fig. 3F) meant that the probe could not be anally inserted. Therefore, consistent placement was achieved using a sterile 2 mm diameter steel rod that was inserted approximately 50 mm into the gut *via* the anus; the rod could be felt through the dermis and an incision was made to allow probe 3 to be inserted

into the intestine laterally. Probe 4 was inserted into epaxial muscle outside of the coelom (body cavity); the incision through the dermis and muscle wall was made approximately 10 mm anterior of the tail, above the lateral line. Other organs, such as the kidney, and gonads (which are typically not known to phosphatize) are too small to reliably insert a probe.

During the primary experiment, the probes were inserted into the organs following this protocol (Fig. 3C). Previous decay experiments have shown that carcasses with compromised dermal integrity decay more rapidly, probably due to increased microbial invasion (see Clements *et al.* 2017). Therefore, silicone grease (Ambersil M494) was injected into each incision around the shaft of the probes, sealing the wound. We ran preliminary experiments using six sea bass carcasses (three without incisions and three with silicone infilled incisions) and found no observable difference in the timing of character loss or disarticulation. The silicone grease also acts to minimize movement of the probe head during decay which can cause the tearing of tissues (Fig. 3D). Extra grease was used on the external dermis around the incisions, as tissue shrinkage in the trials was found to be problematic (Fig. 3E).

After inserting the probes and sealing with grease, the fish carcass was suspended in 1.5 mm plastic mesh netting (per Sansom *et al.* 2010; Fig. 3F) in a plastic frame (Fig. 3G – length 50 cm, width 15 cm, height 15 cm). Probe 5 was placed externally of the carcass, approximately 1–2 mm away from the dermis (see Sagemann *et al.* 1999; Fig. 3G). All probes were attached to the plastic frame to stabilize

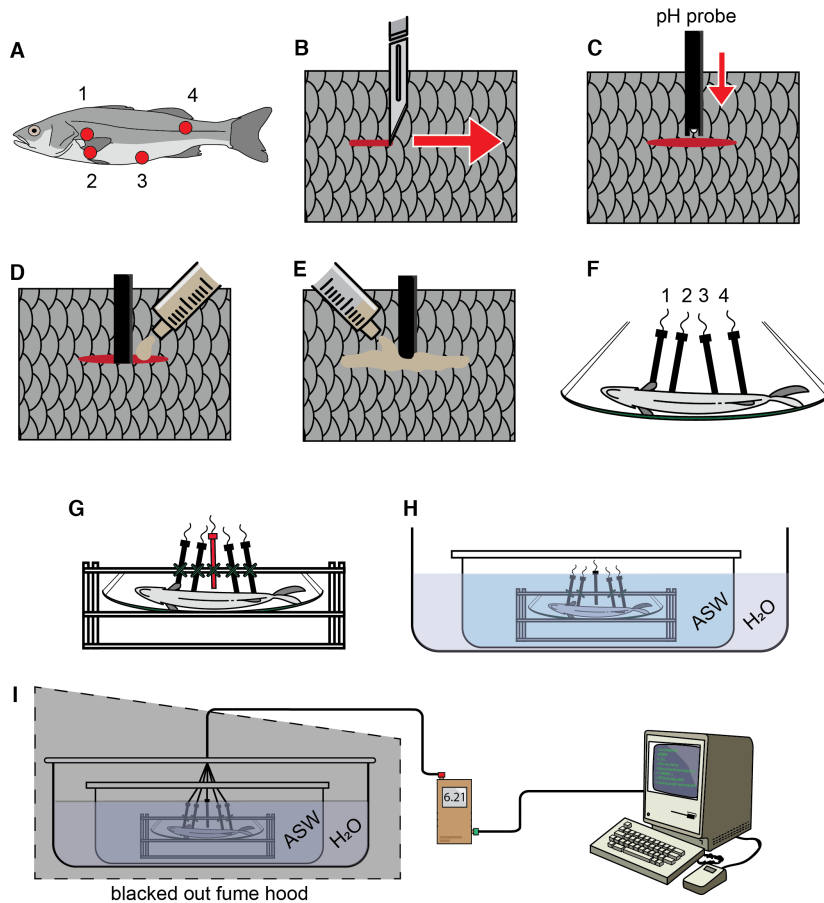


**FIG. 3.** Experimental set-up for monitoring pH in real time inside a carcass. A, four regions to be probed were identified on the sea bass carcass: (1) stomach; (2) liver; (3) intestines; and (4) epaxial muscle mass. B, a 20 mm incision was made in the dermis and down into the cavity; any ribs encountered along the length of the incision were cut. C, the probes were inserted into the appropriate organ. D, inert silicone grease was injected into the incision, around the pH probe shaft, sealing the internal cavity. E, extra silicone grease was used to account for shrinkage during decay. F, the carcass was placed on top of inert plastic netting that allowed the carcass to be removed at the termination of the experiment. G, the netting was suspended in an inert plastic frame which the probes were attached to; this prevented them ripping through the carcass during bloating; a pH probe was placed outside the carcass to log external pH (highlighted red). H, the frame was placed into a plastic box filled with artificial sea water (ASW); this box was then placed within a larger water bath filled with tap water, which acted to reduce temperature variations; there was no water mixing between these two containers and they were sealed with their own lids. I, each probe was plugged into a separate reader device; the five reader devices were connected to a linux OS computer; the computer collected data from each reader device every half hour for the duration of the experiment; the experiment was then sealed and placed within a fume hood and covered from sunlight (to prevent the growth of photosynthesizing organisms).

them and prevent them from rupturing the carcass during the ‘bloat and float’ phase of decay when the build-up of gas within the carcass caused a degree of vertical movement, despite this largely being prevented by plastic netting (Fig. 3G). The carcass, with probes inserted, was placed into a 15 l container (pre-cleaned with alcohol and antibacterial wipes) which was then filled with artificial sea water (Tropic Marin mixed with distilled water) with a salt content of 33–36 ppm, pH 8.

The container was seated within a larger water bath to mitigate temperature fluctuations, and both containers were then sealed with their own lids; there was no

mixing of water during the experiment (Fig. 3H). The experiment was undertaken at ambient room temperature, which for the duration of the experiment measured at 20–23°C. It is important to note that this experiment did not attempt to actively promote mineral replacement of tissues, only to monitor changes in pH arising from autolysis and decay mediated by autochthonous bacteria. As such, unlike previous experiments in which mineralization of tissues was the focus, the artificial sea water was not spiked with calcium or phosphate salts or bacterial inoculum (i.e. Briggs & Kear 1993; Sagemann *et al.* 1999).

The experiment was undertaken inside a fume hood, with a blackout curtain to prevent the growth of photosynthetic organisms. The pH probes were each connected independently to an electronic 'reader' (JENCO 6230N) and calibrated immediately prior to each experiment. The readers were plugged into a USB super-hub via RS232 cables and then connected to a computer. Data was logged every half hour automatically and transposed in MS Excel (Fig. 3I). The experiment ran undisturbed for 65 days. As we only had one set of probes, each of the four probed carcasses were run sequentially (referred to as an 'experimental run'). After each experimental run was terminated, the probes were removed, cleaned with alcohol, recalibrated using pH 4 and pH 7 solution, and left to soak in distilled water for one week. The probes were also recalibrated immediately prior to the commencement of the next experimental run.

Our experimental design aimed to minimize variables between runs. However, there were some uncontrolled variables. As stated earlier, the interval between death of each fish and the start of the experiment was unknown. However, because the fish were stored on ice (but not frozen) immediately after being caught until the start of the experiment, the effects of variable time post mortem should have been minimized. In addition, we cannot rule out microbiome variability across fish.

The protocol for the secondary experiment (which observed the morphological effects of decay on fish carcasses) followed an identical set-up as our pH experiments. Fifteen sea bass specimens, without incisions or probes, were placed individually into containers containing artificial sea water. These containers were also placed into larger water baths (as above) and left inside a blacked-out fume hood. The setting up of the experiment defined day zero, and a single fish carcass was removed and dissected to observe the decay of the internal organs on days: 1, 2, 3, 4, 5, 8, 10, 15, 20, 25, 30, 40, 50, 60 and 70.

*Institutional abbreviations.* BPM, Back to the Past Museum, Cancun, Mexico; CNPEM, Brazilian Center for Research in Energy and Materials; MNCN, Museo Nacional de Ciencias Naturales, Madrid, Spain; NHMUK: Natural History Museum, London, UK.

## RESULTS

### *Decay of external morphology*

Decay data collected from the sea bass carcasses that were not probed (Fig. 4) revealed that within 24 h of the experiment commencing, the normally white ventral flesh became a dull yellow and some scales began to flake away

from the body (Fig. 4B). The carcass began to bloat and if the mouth was closed at the start of the experiment, gas build up could force it open, allowing the gas to escape. If the mouth was not forced open, gas escaped from the operculum. In most samples, the fish began to flex laterally with the head and tail arching toward the water surface, possibly caused by varying decay resistance of soft tissues and build-up of decay gases (see Pan *et al.* 2019). On day six to seven, brown, foul smelling film of adipocere (bacterially-hydrolysed fat) appeared on the water surface. From day zero to this time the water became progressively murkier, often obscuring the decaying carcass. Around day seven, carcasses began to bloat, and the number of shed scales increased (Fig. 4C). At this stage, the gill filaments appeared gelatinous with the lamellae having lost much of their structure.

By day 10, the laterally curled fish had straightened (most likely caused by the decay of muscles) and carcass bloating had increased, with bubbles that smelt of ammonia becoming trapped in the adipocere film on the water surface (Fig. 4D). Around this time the eyeballs began to bulge and show signs of disintegration (the dermal corneal layer split rapidly). Disturbance of the carcass resulted in escape of bubbles from the anus and operculum. From day 16–20, the body cavity began to split, mainly around the anus or at the base of the ribcage, where the ribs would tear through the sagging dermis (Fig. 4E). From these tears a black fluid with mucus-like consistency seeped from the carcass and settled on the bottom of the tank. By day 21, the eyeballs commonly ruptured. It is unclear where these ruptures originated, but the decay gases often forced tears at the edge of the cornea. Through these tears, gas and vitreous humour would escape. In some samples the lens was observed to have detached by day 20.

By day 20, the integrity of the body began to fail. Small breaks in the dorsal dermis appeared, although these did not expose much underlying tissue; by day 26–30, the dermis across the whole carcass showed many lesions, with the dermis shrivelling and receding, exposing internal muscle tissues which had the appearance of a gelatinous white mass with no visible structure (Fig. 4F). Sagging dermis also caused the operculum to open, exposing the remains of the gill structures. Disarticulation of the dorsal and pectoral fins from the carcass occurred after 30 days, however, the tail fin remained attached to the carcass until complete carcass disarticulation. By day 70, the carcass had disarticulated, leaving fragments of skin, scales, gelatinous white matter, bones, and some intact fin rays (Fig. 4G). Even though the fish was in a sealed container, undisturbed and not exposed to water movement, after 70 days of decay the skeleton of the fish was often poorly articulated. The sequence of these events was consistent across the observed fish carcasses (Fig. 4).

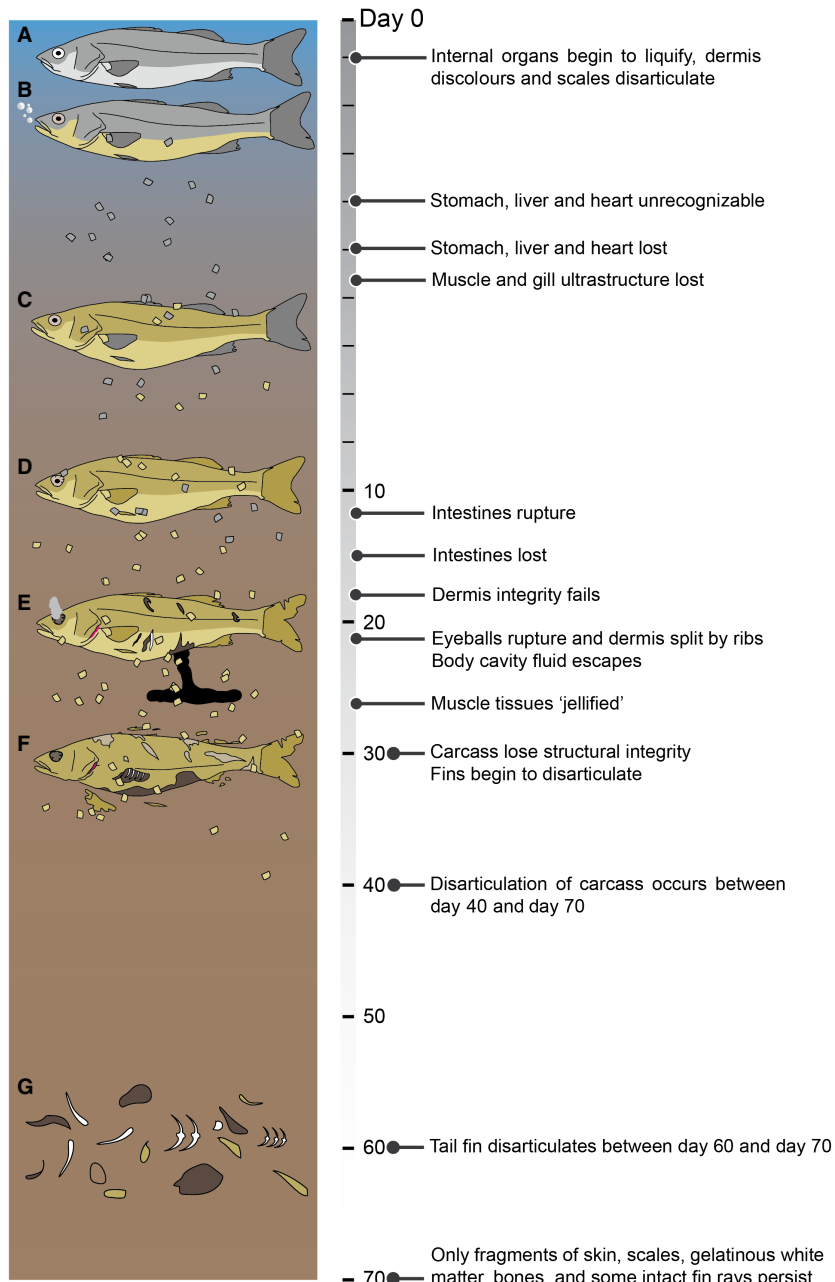


**FIG. 4.** The internal and external decay of a sea bass (*Dicentrarchus labrax*) carcass and a schematic of the surrounding water colour. A, the sea bass carcass is submerged in artificial sea water. B, within 24 h the dermis changes colour to pallid yellow; bloating observed and decay gases escape from orifices such as the mouth and anus; carcass begins to flex laterally. C, carcass bloats further; scales begin to disarticulate from the carcass; water colour turns murky brown and a thick adipocere film forms on the water surface. D, carcass straightens (decay of muscle tissues occurs, counteracting lateral flexing) and bloats further; eyes begin to lose structural integrity. E, splits in the dermis are observed around the anus and around the terminations of the ribs which occasionally tear through the coelom wall; this allows body cavity fluids (a dark viscous liquid) to escape and sink toward the bottom of the container; eyeballs also rupture. F, dermis across the whole carcass wrinkles, splits and recedes, exposing internal flesh; muscle tissues 'jellify' into a gelatinous white mass with no visible structure. G, carcass disarticulation occurs; some fin rays remain mutually articulated and the skeleton is poorly articulated.



*Internal morphological decay*

Typically, within 78–96 h, the stomach, heart and the liver decayed to the extent that we were unable to identify clear morphological details internally or externally; by day 5, organs had fully broken down and formed a dark-coloured, viscous, gelatinous fluid that was denser than the artificial sea water. Determining the exact time that the liver and stomach decayed fully was problematic because removing the carcass caused agitation, making it unclear whether larger fragments seen suspended in the water were the result of disarticulation during decay, or the carcass being removed from the artificial sea water. If the carcass remained undisturbed, this dense dark fluid escaped through fissures in the dermis between day 15 and day 20, and sank to the bottom of the tank.

However, the most persistent internal organ was the intestine (Fig. 4). At day 9, when the other organs were fully disarticulated, the intestine was intact (although it showed evidence of integumentary breakdown at both the stomach and anal terminations). By day 11–12, small ruptures occurred along the main intestinal wall, at which point the integrity of the intestine became compromised and full disarticulation occurred rapidly. Complete loss of the intestine was seen by day 14. The persistence of the intestine is probably due to its robust structure combined with strong muscular sphincters which act to compartmentalize it during early decay. Interestingly, fossil fish ‘intestines’ are often not preserved completely; the sphincter areas where the midgut meet the stomach or the anal end of the hindgut are commonly absent in fossils (Davesne *et al.* 2018).

*pH external to the carcass*

The median pH of the artificial sea water surrounding the carcass fell from pH 8 to below pH 6.38 (the carbonic acid dissociation constant) by day 2 (pH 6.21), remaining below the carbonic acid dissociation constant for just under 19 days (Fig. 5A, F).

After the initial sudden decrease, between day 5 and day 10, the median pH fell to its lowest (pH 6.06) before increasing steadily for the remainder of the experiment. Around day 20 the pH of the fluid around the carcass breached the threshold of pH 6.38 for a period and continued to rise. In experiments that were not terminated at day 30, the pH continued to rise until it was the same as the pH of the artificial sea water at the start of the experiment. In one experiment (experimental run 2) the pH did not fall below the carbonic acid dissociation constant (pH 6.38) but decreased to a minimum of pH 6.56 (Fig. 5F; Clements *et al.* 2022). This is interesting because

the pH of the probed internal organs in the same experiment all reached a pH of 6.38 within 2–3 days.

*pH within the carcass*

At the start of the experiment, the organs within the coelom, the stomach, liver and intestines all had a pH lower than the starting pH of the artificial sea water (pH 8), below the carbonic acid dissociation constant of pH 6.38 (Fig. 5B–D). This is also true of the epaxial muscles (Fig. 5E). This is pertinent, because our data indicate that all probed internal organs (and muscles) generate a pH amenable for phosphatic replacement extremely rapidly (within 24 h of the experiment commencing).

We had expected that the stomach would have had the lowest starting pH of the internal organs due to the presence of gastric acids, however, our data show that this was not the case. Studies using *Diplodus sargusi* (white seabream), demonstrated that prior to ingesting food, the stomach pH was close to 7, however, approximately four hours after eating, the stomach pH had values under 4, with the lowest pH (>pH 3) occurring eight hours after eating as a direct response to ingestion of food (Yúfera *et al.* 2012). Although inter-taxonomic variation in stomach pH cannot be discounted, it may be possible that the sea bass used in this experiment had not eaten recently before being caught or had emptied their stomachs due to the trauma of being caught; fish are commonly observed to regurgitate food when stressed, especially during trawling (Staniland *et al.* 2001).

The median pH values for the liver, stomach and intestines show similar general trends during decay (Fig. 5A). There is a slight decrease for several days, before the pH plateaus, well below the carbonic acid dissociation constant (pH 6.38), from day 12–16. At this point, the pH for all three organs began to rise, presumably as the decay fluid homogenizes within the coelomic cavity. By day 30, the pH of the stomach, liver and intestines was above the carbonic acid dissociation constant of pH 6.38. The pH of the three organs continued to rise; in experiments that ran until complete disarticulation, the pH of the organs equilibrated with the external pH after the body cavity ruptured. Importantly for the potential for phosphatic precipitation, the median pH of each organ was below the pH 6.38 threshold before day 5, prior to disarticulation. Despite not being within the coelom, the epaxial muscles had a similar pH trajectory as the internal organs (stomach, intestines and liver) although the pH values were elevated compared to those of internal organs (Fig. 5A).

The internal organs showed variability in pH across the four specimens. Of the internal organs probed, the stomach had the least variation in pH between specimens but

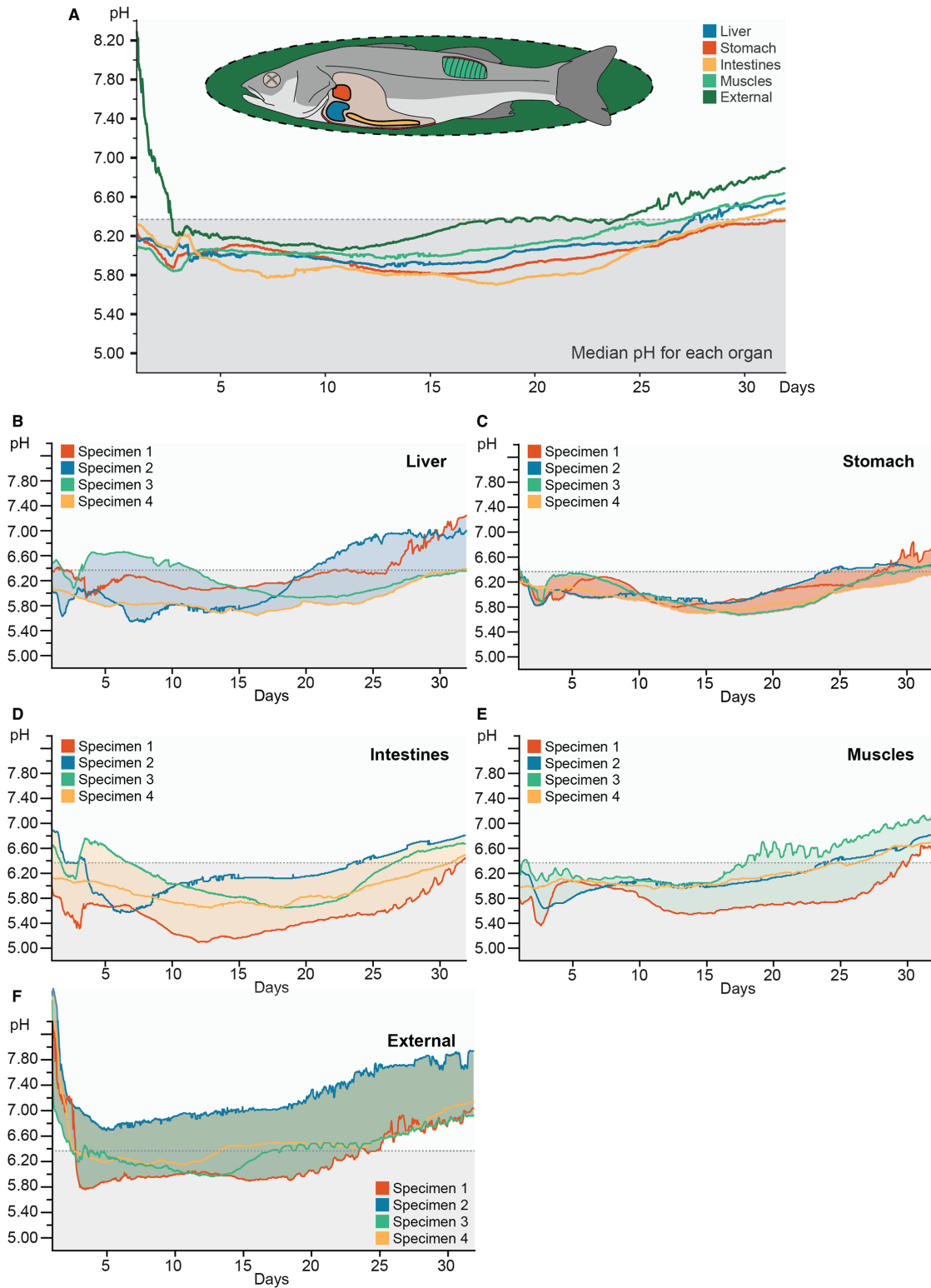


**FIG. 5.** Internal pH of a decaying sea bass (*Dicentrarchus labrax*) carcass (n = 4). A, the median pH of each probed organ for four specimens. B–F, the pH trajectory of each organ for the four specimens; the infilled coloured areas represent the maximum pH range; the data were collected until the body cavity ruptured after 30 days; grey shaded area below dotted line represents the pH window for calcium phosphate precipitation (i.e. below the carbonic acid dissociation constant pH 6.38).

both the liver and intestines experienced pH variability between specimens. In specimen 3 a sudden pH elevation was recorded around day 4 in all the organs, although to varying intensities. At the start of the experiment, specimen 3 showed a drop in pH in all organs, however, the liver and intestine pH increased suddenly above the carbonic acid dissociation constant (intestine pH 6.63 and liver pH 6.53). This was higher than the external pH at the time (pH 6.22–6.32). The stomach also showed a rise in pH but did not breach the carbonic acid dissociation constant. The intestine's pH stayed above the carbonic acid dissociation constant for about 48 h whereas the liver remained above pH 6.38 for over 6 days. This rise in pH was not observed in the epaxial muscles in specimen 3. It is unclear what caused this.

Specimen 1 also yielded interesting results as the pH of the liver and stomach during days 3–10 was higher than the external pH of the carcass (on day 5: liver pH 6.19, stomach pH 6.18, external pH 5.98). However, this pH elevation did not raise any of the organ's pH above of the carbonic acid dissociation constant.

In specimen 1, small-scale pH spikes were observed in the external pH and to a lesser extent the intestines after day 25. In specimen 3, pH fluctuations of a similar small-scale were recorded at day 17 in the external probe and epaxial muscles (close to the dermis). It is unclear what caused these pH spikes. It is unlikely that these spikes were caused by external water entering the carcass, because that would cause the pH conditions to equilibrate with the external pH. One explanation is that the spikes record differences in bacterial respiration rates across day and night cycles (possibly caused by temperature fluctuation).

## DISCUSSION

Our investigation provides the first record of dynamic pH gradients inside a carcass during the early stages of decay. The decreasing pH gradients observed external to the sea bass carcasses conformed with pH gradients seen in previous decay experiments on other fish taxa such as mackerel and sprats, as well as arthropods and non-decabrachian cephalopods (Sagemann *et al.* 1999; Clements *et al.* 2017). However, our data demonstrates that, at least whilst the dermis is intact, the pH inside a fish carcass is lower than the pH immediately outside of the carcass. This is not surprising but because phosphatization is controlled by pH it is important, emphasizing the need to document decay-induced pH gradients within the carcass at a fine spatial resolution.

We were unable to reject our second null hypothesis; within the coelom, each individual organ did not generate a unique pH profile. Rather, the decay of internal organs

contributes to the formation of a pervasive pH environment throughout the body cavity. This pervasive pH environment persists until the dermis ruptures. When this happens the organs in the coelom are no longer in a 'compartment' (i.e. a microenvironment) within the fish, and consequently the pH within the fish rapidly equilibrates with the pH recorded in ambient external conditions, probably owing to both the escape of fluids from within the body, and the ingress of saltwater into the body. This raises the question: if, during decay, all internal organs within the coelom are inside a pH environment below the carbonic acid dissociation constant (pH 6.38), why are some internal organs consistently preserved in calcium phosphate in exceptionally preserved fossils, whilst others are lost?

Our data indicate that we can discount differences in tissue decay rate: most of the internal organs (i.e. stomach, liver, heart, gonads, kidney) became unrecognizable within just five days post mortem, and the gills and muscles lost their structure 24 h later (the flexing of the fish within 24 h of the experiment starting suggests that muscular decay begins rapidly). The intestine persisted for a slightly longer period, being lost at around 10–14 days. Within this highly condensed timeframe between death and complete decay, there is no correlation between the timing of loss of organs and their likelihood of occurrence in the phosphatic fossil record; commonly phosphatized internal organs are not the most persistent organs.

There is some experimental evidence to indicate that endogenous bacteria may promote preservation of internal organs, perhaps even selectively, through the creation of bacterial biofilms which pseudomorph anatomy (Butler *et al.* 2015) and/or the formation of substrates suitable for mineralization (e.g. Raff *et al.* 2008). We did not observe bacterial biofilm pseudomorphs of any internal organs within the fish carcasses, which accords with the view of Butler *et al.* (2015) that the scale of an organism may be a limiting factor (however, we did not examine these tissues with electron microscopy). Furthermore, as epaxial muscles are also commonly phosphatized but outside of the coelom, it is unlikely that gut microbes are responsible for colonizing these tissues. However, our experiments were not designed to explore the role of endogenous bacteria during decay/preservation, and this is likely to be an important area for future study.

One of the critical controls on the balance of outcomes from decay and mineralization is the abundance of mineralizing ions, and in the context of soft-tissue phosphatization (especially in marine waters) the limiting ion is phosphate ( $\text{PO}_4^{3-}$ ) (Briggs & Kear 1994; Sagemann *et al.* 1999). Experiments on crustaceans have confirmed that phosphate ions are liberated from the decay of tissues (Briggs & Kear 1993, 1994; Wilby & Briggs 1997) predominantly through the breakdown of phospholipids,

nucleotides and adenosine triphosphate (ATP) (Briggs & Kear 1993, 1994; Wilby & Whyte 1995; Wilby & Briggs 1997; McNamara *et al.* 2009; Lerosey-Aubril *et al.* 2012). Importantly, phosphate content is highly variable across organs and this may account for selective phosphatization (e.g. Mitchell *et al.* 1945).

Decaying muscles are rich in phosphates (i.e. ATP) and our data show that they can rapidly generate a pH microenvironment within the dermis that is amenable to phosphatization. Muscle tissues also contain large quantities of collagen, which has been found to actively induce calcium phosphate precipitation and act as substrate for mineralization (for a review of this phenomenon see McNamara *et al.* 2009). This may explain why muscles are the most frequently occurring phosphatized soft tissues in the fossil record with instances across many taxa and deposits (e.g. Allison 1988; Wilby & Whyte 1995; Wilby & Briggs 1997; Wilson *et al.* 2016; Clements *et al.* 2017; Table S1) although variations in the phosphatization potential of different muscle tissue has been suggested (Wilson *et al.* 2016).

The other major internal organs (i.e. stomach, liver, intestines, gonads, kidneys) contain less tissue-bound phosphate compared to muscles (e.g. Mitchell *et al.* 1945). This suggests that the liberation of tissue-bound phosphate ions during decay cannot explain the frequency with which stomachs and intestines are preserved in calcium phosphate (e.g. Martill 1988; Wilby & Martill 1992; Orr *et al.* 2000; Etter & Tang 2002; McNamara *et al.* 2009; Lerosey-Aubril *et al.* 2012; Maldanis *et al.* 2016; Zacaí *et al.* 2016). However, it is important to note that preservation of the stomach and intestine integument is generally rare; most records reflect the preserved remains of the contents of these organs (i.e. undigested organic matter). For example, in fossil fish from the Santana Formation the 'guts' primarily comprise preserved gut contents, with little of the stomach/intestine integument remaining (Wilby & Martill 1992). In fossil frogs from the Libros (Upper Miocene, Spain), calcium phosphate occurs as void fill within the stomach (McNamara *et al.* 2009). There is no evidence that phosphate had diffused through the stomach wall from another tissue source; the phosphate was sourced from consumed organic matter (McNamara *et al.* 2009). If this is the case, the enhanced likelihood of phosphatic replacement of the stomach and/or intestine contents (and more rarely the integument) may be controlled by the composition of the contents (e.g. muscle, bone, plant matter, algae) from which phosphate can be liberated during early mineralization. The requirement for supplementary ingested organics would also explain why in some Lagerstätte, preservation of these organs is not consistent within a taxon (e.g. Wilby & Martill 1992).

## CONCLUSION

Our experiments show that, during decay, a pH that favours phosphatization develops rapidly and pervasively inside sea bass carcasses. Our data provide no support for the hypothesis that spatially distinct pH microenvironments associated with specific organs develop during decay, suggesting that other factors are more important in controlling which organs are replaced through phosphatization. We hypothesize that, once pH requirements are met, it is the biogenic phosphorus content of organs that plays a role in selective phosphatization. Organs with a high phosphate content (and those rich in collagen) and those in proximity to a source of phosphorus which can be rapidly liberated on decay, such as the contents of stomach and intestine, are selectively phosphatized. Organs that lack sufficient tissue-bound phosphorus will not be phosphatized and, unless stabilized by other modes of preservation during decay and diagenesis, will be lost. Compositional heterogeneity across organs has the potential to control their selective mineralization and this may extend beyond the phosphatization taphonomic mode. For example, rapid availability of iron from a biogenic source is important in selective preservation of some soft tissues by iron mineralization of non-biomineralized tissues in the Cambrian Chengjiang and Ordovician Fezouata Lagerstätten (Saleh *et al.* 2020).

Currently, our data is limited to a fish taxon. Undertaking experiments to log internal chemical changes during decay is difficult, expensive and time consuming, but as technological advances continue and probes become smaller, cheaper and more robust, we recommend further experimentation using other taxa (arthropods, amphibians etc.) to expand our understanding of phosphatic mineral replacement. A complementary avenue of investigation would be to record Eh (oxidation potential) as well as pH, allowing an in-depth investigation into the stability of calcium phosphate during the decay of a carcass. Our data also indicate that experimental designs that only use external conditions as a pH proxy for internal conditions within a carcass should be interpreted cautiously.

*Acknowledgements.* Yu Jing and Gina Lewis are thanked for helping with the experimental set-up and dissections. Richard Moore for writing the script for the linux machine. Paddy Orr and Mark Williams for their constructive feedback during TC's PhD viva examination. The Leicester University Palaeobiology, Palaeoenvironments & Palaeoclimates Research Group is thanked for constructive feedback. Rudy Lerosey-Aubril and Donald Davesne for discussion on aspects of the manuscript. A. Clements and E. Dunne are thanked for proof reading. SEG thanks the School of Geography, Geology and Environment, University of Leicester for funding the purchase of the pH

probes. Experiment was undertaken as part of a Natural Environment Research Council studentship NE/L501839/1 (to TC). TC is currently supported by a Leverhulme Early career Fellowship (ECF-2019-097). We also thank Philip Wilby and Maria McNamara for reviews.

*Author contributions.* **Conceptualization** Sarah Gabbott (SG), Thomas Clements (TC); **Data Curation** TC, SG; **Formal Analysis** TC, SG, Mark A. Purnell (MAP); **Funding Acquisition** SG, MAP; **Investigation** TC, SG; **Methodology** TC, SG; **Project Administration** TC, SG; **Resources** SG, MAP; **Software** Alan Moore (University of Leicester); **Supervision** SG, MAP; **Validation** SG, MAP; **Visualization** TC; **Writing – Original Draft Preparation** TC, SG; **Writing – Review & Editing** TC, SG, MAP.

## DATA ARCHIVING STATEMENT

Data for this study are available in the Dryad Digital Repository: <https://doi.org/10.5061/dryad.k6djh9w8n>

*Editor.* Paul Smith

## SUPPORTING INFORMATION

Additional Supporting Information can be found online (<https://doi.org/10.1111/pala.12617>):

**Table S1** Examples of phosphatic fossil beds.

## REFERENCES

- ALLISON, P. A. 1988. Phosphatized soft-bodied squids from the Jurassic Oxford Clay. *Lethaia*, **21**, 403–410.
- ARENA, D. A. 2008. Exceptional preservation of plants and invertebrates by phosphatization, Riversleigh, Australia. *PALAIOS*, **23**, 495–502.
- BRIGGS, D. E. G. 2003. The role of decay and mineralization in the preservation of soft-bodied fossils. *Annual Review of Earth & Planetary Sciences*, **31**, 275–301.
- BRIGGS, D. E. G. and KEAR, A. J. 1993. Fossilization of soft tissue in the laboratory. *Science*, **259**, 1439–1442.
- BRIGGS, D. E. G. and KEAR, A. J. 1994. Decay and mineralization of shrimps. *PALAIOS*, **9**, 431–456.
- BRIGGS, D. E. G. and WILBY, P. R. 1996. The role of the calcium carbonate-calcium phosphate switch in the mineralization of soft-bodied fossils. *Journal of the Geological Society*, **153**, 665–668.
- BRIGGS, D. E. G., KEAR, A. J., MARTILL, D. M. and WILBY, P. R. 1993. Phosphatization of soft-tissue in experiments and fossils. *Journal of the Geological Society*, **150**, 1035–1038.
- BUTLER, A. D., CUNNINGHAM, J. A., BUDD, G. E. and DONOGHUE, P. C. 2015. Experimental taphonomy of *Artemia* reveals the role of endogenous microbes in mediating decay and fossilization. *Proceedings of the Royal Society B*, **282**, 20150476.
- BUTTERFIELD, N. J. 2002. *Leaenchoilia* guts and the interpretation of three-dimensional structures in Burgess Shale-type fossils. *Paleobiology*, **28**, 155–171.
- CLEMENTS, T., COLLEARY, C., DE BAETS, K. and VINTHER, J. 2017. Buoyancy mechanisms limit preservation of coleoid cephalopod soft tissues in Mesozoic Lagerstätten. *Palaeontology*, **60**, 1–14.
- CLEMENTS, T., PURNELL, M., GABBOTT, S. 2022. Data from: Experimental analysis of organ decay and pH gradients within a carcass and the implications for phosphatization of soft tissues. *Dryad Digital Repository*. <https://doi.org/10.5061/dryad.k6djh9w8n>
- DAVESNE, D., GUERIAU, P., DUTHEIL, D. B. and BERTRAND, L. 2018. Exceptional preservation of a Cretaceous intestine provides a glimpse of the early ecological diversity of spiny-rayed fishes (Acanthomorpha, Teleostei). *Scientific Reports*, **8**, 8509.
- DUNCAN, I. J., BRIGGS, D. E. and ARCHER, M. 1998. Three-dimensionally mineralized insects and millipedes from the Tertiary of Riversleigh, Queensland, Australia. *Palaeontology*, **41**, 835–852.
- ETTER, W. and TANG, C. M. 2002. Posidonia shale: Germany's Jurassic marine park. 265–291. In BOTTJER, D. J., ETTER, W., HAGADORN, J. W. and TANG, C. M. (eds) *Exceptional fossil preservation: A unique view on the evolution of marine life*. Columbia University Press.
- FUCHS, D., WILBY, P. R., VON BOLETZKY, S., ABISAAD, P., KEUPP, H. and IBA, Y. 2016. A nearly complete respiratory, circulatory, and excretory system preserved in small Late Cretaceous octopods (Cephalopoda) from Lebanon. *Paläontologische Zeitschrift*, **90**, 299–305.
- INIESTO, M., LAGUNA, C., FLORÍN, M., GUERRERO, M. C., CHICOTE, A., BUSCALIONI, A. D. and LOPEZ-ARCHILLA, A. I. 2015. The impact of microbial mats and their microenvironmental conditions in early decay of fish. *PALAIOS*, **30**, 792–801.
- LEROSEY-AUBRIL, R., HEGNA, T. A., KIER, C., BONINO, E., HABERSETZER, J. and CARRÉ, M. 2012. Controls on gut phosphatization: the trilobites from the Weeks Formation Lagerstätte (Cambrian; Utah). *PLoS One*, **7**, e32934.
- MALDANIS, L., CARVALHO, M., ALMEIDA, M. R., FREITAS, F. I., DE ANDRADE, J. A. F. G., NUNES, R. S., ROCHITTE, C. E., POPPI, R. J., FREITAS, R. O. and RODRIGUES, F. 2016. Heart fossilization is possible and informs the evolution of cardiac outflow tract in vertebrates. *eLife*, **5**, e14698.
- MARTILL, D. M. 1988. Preservation of fish in the Cretaceous Santana Formation of Brazil. *Palaeontology*, **31**, 1–18.
- McNAMARA, M. E., ORR, P. J., KEARNS, S. L., ALCALÁ, L., ANADÓN, P. and PEÑALVER MOLLA, E. 2009. Soft-tissue preservation in Miocene frogs from Libros, Spain: insights into the genesis of decay microenvironments. *PALAIOS*, **24**, 104–117.
- McNAMARA, M. E., ORR, P. J., ALCALÁ, L., ANADÓN, P. and PEÑALVER, E. 2012. What controls the taphonomy

- of exceptionally preserved taxa—environment or biology? A case study using frogs from the Miocene Libros Konservat-Lagerstätte (Teruel, Spain). *PALAIOS*, **27**, 63–77.
- McNAMARA, M. E., ORR, P. J., KEARNS, S. L., ALCALÁ, L., ANADÓN, P. and PEÑALVER, E. 2016. Reconstructing carotenoid-based and structural coloration in fossil skin. *Current Biology*, **26**, 1075–1082.
- MITCHELL, H., HAMILTON, T., STEGGERDA, F. and BEAN, H. 1945. The chemical composition of the adult human body and its bearing on the biochemistry of growth. *Journal of Biological Chemistry*, **158**, 625–637.
- ORR, P. J., BRIGGS, D. E., SIVETER, D. J. and SIVETER, D. J. 2000. Three-dimensional preservation of a non-biom mineralized arthropod in concretions in Silurian volcaniclastic rocks from Herefordshire, England. *Journal of the Geological Society*, **157**, 173–186.
- PAN, Y., FÜRSICH, F. T., CHELLOUCHE, P. and HU, L. 2019. Taphonomy of fish concentrations from the Upper Jurassic Solnhofen Plattenkalk of Southern Germany. *Neues Jahrbuch für Geologie und Paläontologie*, **292**, 73–92.
- PURNELL, M. A., DONOGHUE, P. J., GABBOTT, S. E., McNAMARA, M. E., MURDOCK, D. J. and SANSOM, R. S. 2018. Experimental analysis of soft-tissue fossilization: opening the black box. *Palaeontology*, **61**, 317–323.
- RAFF, E. C., SCHOLLAERT, K. L., NELSON, D. E., DONOGHUE, P. C., THOMAS, C. W., TURNER, F. R., STEIN, B. D., DONG, X., BENGTSON, S., HULDTGREN, T. and STAMPANONI, M. 2008. Embryo fossilization is a biological process mediated by microbial biofilms. *Proceedings of the National Academy of Sciences*, **105**, 19360–19365.
- SAGEMANN, J., BALE, S. J., BRIGGS, D. E. and PARKES, R. J. 1999. Controls on the formation of authigenic minerals in association with decaying organic matter: an experimental approach. *Geochimica et Cosmochimica Acta*, **63**, 1083–1095.
- SALEH, F., DALEY, A. C., LEFEBVRE, B., PITTET, B. and PERRILLAT, J. P. 2020. Biogenic iron preserves structures during fossilization: a hypothesis: iron from decaying tissues may stabilize their morphology in the fossil record. *BioEssays*, **42**, 1900243.
- SANSOM, R. S., GABBOTT, S. E. and PURNELL, M. A. 2010. Non-random decay of chordate characters causes bias in fossil interpretation. *Nature*, **463**, 797–800.
- STANILAND, I., HART, P. and BROMLEY, P. 2001. The regurgitation of stomach contents in trawl caught whiting, evidence of a predator size effect. *Journal of Fish Biology*, **59**, 1430–1432.
- WILBY, P. 1993. The role of organic matrices in post-mortem phosphatization of soft tissues. *Kaupia*, **2**, 99–113.
- WILBY, P. R. and BRIGGS, D. E. 1997. Taxonomic trends in the resolution of detail preserved in fossil phosphatized soft tissues. *Geobios*, **30**, 493–502.
- WILBY, P. R. and MARTILL, D. M. 1992. Fossil fish stomachs: a microenvironment for exceptional preservation. *Historical Biology*, **6**, 25–36.
- WILBY, P. R. and WHYTE, M. A. 1995. Phosphatized soft tissues in bivalves from the Portland Roach of Dorset (Upper Jurassic). *Geological Magazine*, **132**, 117–120.
- WILBY, P. R., BRIGGS, D. E., BERNIER, P. and GAILLARD, C. 1996. Role of microbial mats in the fossilization of soft tissues. *Geology*, **24**, 787–790.
- WILBY, P., HUDSON, J., CLEMENTS, R. and HOLLINGWORTH, N. 2004. Taphonomy and origin of an accumulate of soft-bodied cephalopods in the Oxford Clay Formation (Jurassic, England). *Palaeontology*, **47**, 1159–1180.
- WILSON, P., PARRY, L. A., VINTHER, J. and EDGE-COMBE, G. D. 2016. Unveiling biases in soft-tissue phosphatization: extensive preservation of musculature in the Cretaceous (Cenomanian) polychaete *Rollinschaeta myoplana* (Annelida: Amphinomididae). *Palaeontology*, **59**, 463–479.
- YÚFERA, M., MOYANO, F. J., ASTOLA, A., POUSSÃO-FERREIRA, P. and MARTÍNEZ-RODRÍGUEZ, G. 2012. Acidic digestion in a teleost: postprandial and circadian pattern of gastric pH, pepsin activity, and pepsinogen and proton pump mRNAs expression. *PLoS One*, **7**, e33687.
- ZACAÍ, A., VANNIER, J. and LEROSEY-AUBRIL, R. J. A. S. 2016. Reconstructing the diet of a 505-million-year-old arthropod: *Sidneyia inexpectans* from the Burgess Shale fauna. *Arthropod Structure & Development*, **45**, 200–220.